

This is the author's version of a work that was accepted for publication in the Journal Geotextiles and Geomembranes. Changes resulting from the publishing process, such as peer review, editing, corrections, structural formatting and other quality control mechanisms may not be reflected in this document. Changes may have been made to this work since it was submitted for publication. A definitive version was subsequently published in the Journal Geotextiles and Geomembranes, Volume 42, Issue 1, February 2014, Pages 1-14. <http://doi.org/10.1016/j.geotexmem.2013.11.001>

1 **Probabilistic Design of Ground Improvement by**
2 **Vertical Drains for Soil of Spatially Variable Coefficient**
3 **of Consolidation**

4
5 **Md. Wasiul Bari†**

6 Assistant Professor, Department of Civil Engineering,
7 Rajshahi University of Engineering and Technology, Rajshahi 6204, Bangladesh

8 E-mail: wasiul_bari@yahoo.com

9
10
11 **Mohamed A. Shahin**

12 Associate Professor, Department of Civil Engineering,
13 Curtin University, WA 6845, Australia

14 E-mail: M.Shahin@curtin.edu.au

15
16
17 †Corresponding author

18 Submitted to: **Geotextiles and Geomembranes**

29 **Abstract:** The design of soil consolidation via prefabricated vertical drains (PVDs) has
30 been traditionally carried out deterministically and thus can be misleading due to the
31 ignorance of the uncertainty associated with the inherent variability of soil properties.
32 To treat such uncertainty in the course of design of soil improvement by PVDs, more
33 rational probabilistic methods are necessary. In this paper, a simplified probabilistic
34 method is proposed in which the inherent variability of the coefficient of consolidation,
35 which is the most significant uncertain soil parameter that affects the consolidation
36 process, is considered. An easy-to-use design procedure and charts are provided for
37 routine use by practitioners.

38

39 **Keywords:** Probabilistic design; Soil consolidation; Vertical drains; Soil spatial
40 variability.

41

42

43

44

45

46

47

48

49

50

51

52

53 **Introduction**

54

55 Over the past decade or so, the development activities in areas of soft soils have
56 increased significantly so as to suit the demands of the increased population in many
57 countries and to ensure the marginal use of limited land space. Construction over soft
58 soils often requires a pre-construction treatment of the existing soft sub-soils so that soil
59 strength and stiffness are improved, thus, eliminating the undue risks of excessive post
60 construction deformations and associated instability. Among a number of available
61 ground improvement techniques, the use of prefabricated vertical drains (PVDs) with
62 preloading has become the most viable for stabilization of soft soils (Indraratna et al.,
63 2012). PVDs accelerate the consolidation process and prevent post-construction build-
64 up of excess pore water pressure, leading to improved soil strength and reduced lateral
65 and differential settlements (Rowe and Taechakumthorn, 2008).

66

67 Despite the fact that the theoretical design aspects of soil consolidation by PVDs are
68 well established (e.g. Barron, 1948; Hansbo, 1981; Hird et al., 1992; Onoue, 1988;
69 Yoshikuni and Nakanodo, 1974), reliable predictions of the soil consolidation rates
70 remain difficult to obtain due to the uncertainty associated with the factors affecting the
71 consolidation process (Hong and Shang, 1998; Rowe, 1972; Zhou et al., 1999). The
72 uncertainty associated with the design of any geotechnical engineering system including
73 soil consolidation can be divided into three main sources (Phoon and Kulhawy, 1999):
74 inherent variability; measurement error and transformation uncertainty. The inherent
75 variability (also called aleatoric uncertainty) is due to the natural geologic processes
76 caused by the complex characteristics of transport of raw materials, layered deposition

77 and common weathering (Vanmarcke, 1977). The measurement error is mainly due to
78 the inadequate equipment and poor testing procedures. The transformation uncertainty
79 (also called model uncertainty) occurs during the translation of the field or laboratory
80 measurements into design, using empirical or correlation models. Collectively, the
81 measurement error and model uncertainty can be described as epistemic uncertainty. To
82 obtain a reliable design for a geotechnical system, all of the above sources of
83 uncertainty should be taken into consideration. However, the measurement error and
84 transformation uncertainty can be reduced or even removed by improving the
85 measurement methods and enhancing the calculation models (Lacasse and Nadim,
86 1996). Therefore, the inherent variability is the most significant source of uncertainty
87 that needs to be addressed in design of geotechnical engineering systems and this is the
88 main focus of the present paper for soil improvement by PVDs.

89

90 The degree of consolidation achieved via PVDs is greatly controlled by some soil
91 properties (e.g. soil permeability and volume compressibility) that are spatially variable
92 and potentially induce inherent variability in their characterization, which provides
93 significant geotechnical uncertainty. However, given the analytical and numerical
94 complexity of the problem of soil improvement by PVDs, available research into soil
95 consolidation considering geotechnical uncertainty has been very limited and also failed
96 to accommodate the true nature of inherent soil variability. For example, Hong and
97 Shang (1998) and Zhou et al. (1999) presented a probabilistic design method based on
98 available analytical solutions considering the geotechnical uncertainty associated with
99 the coefficient of horizontal (radial) consolidation. However, this method is inadequate
100 as soil variability was characterized by random values rather than by random fields.

101 Walker and Indraratna (2006) proposed an analytical model based on Hansbo (1981)
102 theory incorporating a parabolic horizontal permeability distribution in the smear zone.
103 Basu et al. (2006) and Abuel-Naga et al. (2012) have extended the work done by
104 Walker and Indraratna (2006) to include a transition zone of linearly varying
105 permeability between the smear and undisturbed zones, but the permeability in the
106 smear and undisturbed zones are assumed to be constant. Therefore, there is a need to
107 develop an alternative probabilistic design method that considers the true nature of soil
108 inherent variability in the course of design of soil improvement by PVDs and this paper
109 will fill in this gap.

110

111 In order to include the inherent soil variability in design of soil improvement by PVDs,
112 a computational numerical stochastic scheme that combines the finite element method
113 and Monte Carlo (FEMC) technique can be employed. However, such numerical
114 scheme is complex and requires a large number of simulations that are computationally
115 intensive and time consuming, and it is not uncommon that practicing engineers have
116 neither the time nor the resources to perform such FEMC simulations. Consequently, in
117 this work, an alternative approximate simplified probabilistic design method (PDM) that
118 can be readily used by practitioners is developed in which the inherent soil variability of
119 the coefficient of consolidation is explicitly incorporated in a systematic and
120 economically viable manner. The proposed PDM is verified by comparing its results
121 with those obtained from the FEMC solutions and the results are found to be in good
122 agreement. In the sections that follow, detailed description of the proposed PDM is
123 demonstrated followed by the stochastic FEMC approach. Finally, a comparison
124 between the results obtained from the PDM and FEMC is presented and discussed.

125 **Probabilistic Design Method of Soil Consolidation by PVDs**

126

127 The probabilistic design method (PDM) described herein considers, for the first time,
128 incorporation of the true nature of soil variability in design of soil improvement by
129 PVDs. The soil property considered to be randomly variables is the horizontal
130 coefficient of consolidation, c_h , as it is the most significant soil property that affects soil
131 consolidation by PVDs, as explained in the next section. It should be noted that the
132 proposed PDM method is an extension of the previous work done by Hong and Shang
133 (1998) and Zhou et al. (1999) but in the current study the inherent soil variability of c_h
134 is explicitly incorporated and appropriately implemented. The proposed PDM is
135 approximate and can be used to estimate the drain spacing by employing a factored
136 design value of c_h so as to satisfy a specific target probability level of the degree of
137 consolidation that needs to be achieved in a specified timeframe. The proposed PDM
138 involves the following steps:

- 139 1. Identification and characterization of soil properties that are spatially variable in the
140 ground;
- 141 2. Development of analytical formulation for the design factors taking into account the
142 associated uncertainty due to spatially variable soils;
- 143 3. Estimation of correlation structure of soils; and
- 144 4. Development of probabilistic design procedure and charts for routine use by
145 practitioners.

146 Details of the above steps are described and discussed below.

147

148

149 **Identification and characterization of spatially variable soil properties**

150

151 As mentioned earlier, spatial variability of soil properties affects the behavior of soil
152 consolidation, and among all soil properties affecting soil consolidation, the coefficient
153 of vertical consolidation, c_v , and coefficient of horizontal consolidation, c_h , are the most
154 significant. Both c_v and c_h may vary substantially in the ground, even in a uniform soil
155 layer (Chang, 1985). For example, based on experimental data, Terzaghi et al. (1996)
156 reported that the coefficient of variation (COV) of c_v for Mexico City clay, San
157 Francisco clay and clay deposit in Pisa (Italy) are 12%, 35% and 69%, respectively. By
158 analyzing c_v values obtained from oedometer tests carried out on Kawasaki clay, Chang
159 (1985) estimated COV of c_v to be 30%. According to data reported by Lumb (1974), the
160 COV of c_v and c_h are estimated to range from 25% to 50%, and based on data reported
161 in the literature, Lee et al. (1983) found that the extent to which c_v and c_h vary may
162 range from 25% to 100%.

163

164 As mentioned above, both c_v and c_h exhibit inherent variability and may be considered
165 as random variables in design of soil stabilization by PVDs. However, in accordance
166 with the sensitivity analyses carried out by Hong and Shang (1998) and Zhou et al.
167 (1999) considering several uncertain soil properties, it was found that c_h is the most
168 significant random soil property affecting the degree of soil consolidation by PVDs. In
169 addition, the consolidation of soil by PVDs can take place by simultaneous vertical and
170 horizontal (radial) drainage of water. However, as the drainage length in the vertical
171 direction is significantly higher than that of the horizontal direction and water flow
172 resistance in the horizontal direction is often much lower than that of the vertical

173 direction (Bergado et al., 1993; Hansbo, 1981), soil consolidation due to vertical
174 drainage is much less than that of horizontal drainage. Furthermore, it has been shown
175 by Crawford et al. (1992) from a back-analysis of an instrumented test embankment in
176 Canada that the rates of consolidation are very sensitive to c_h , and that c_h is the most
177 significant design parameter. Accordingly, in the proposed probabilistic design
178 approach, c_h is considered to be the only spatially variable soil property, while the other
179 soil properties are held constant and treated deterministically, including c_v , so as to
180 reduce the superfluous complexity of the problem.

181

182 Inherent variability of soil properties can be mathematically characterized by treating
183 the soil properties as random variables. In statistics, a random variable is described by a
184 probability distribution (usually referred to as the ‘PDF’ or probability density
185 function). The PDF of a random variable can be represented by several classical
186 statistical parameters, namely, the mean value, μ , variance, σ^2 (the variance can also be
187 represented by standard deviation, σ , or COV, v and $v = \sigma/\mu$). However, inherent
188 variability of soil properties is not entirely random and spatial dependencies also exist
189 (Fenton and Vanmarcke, 1990; Jaksa et al., 1997; Vanmarcke, 1977). That is, a soil
190 property at two separate spatial locations could be similar or otherwise, depending on
191 the distance they are located apart and this is known as spatial correlation. Vanmarcke
192 (1977) pointed out that adequate characterization of spatially variable soil properties
193 requires consideration (incorporation) of such spatial correlation. The mean and
194 standard deviation are the point statistical measures with no consideration of the spatial
195 correlation structure of soil properties. Therefore, a third parameter (i.e. the scale of
196 fluctuation, SOF) is usually introduced as an additional statistic to consider the spatial

197 correlation of soil properties. The scale of fluctuation is also known as the correlation
198 length and is usually denoted as θ . Generally speaking, a large value of θ indicates
199 smooth spatial variation of soil property of interest, whereas a small value of θ implies
200 erratic variation. All soils by nature exhibits SOF due to the geological process of
201 transport of raw materials, layer deposition and common weathering process. An
202 extensive literature review suggested that the amount of information on SOF is
203 relatively limited in comparison to the amount of information on the COV of soil
204 variability. Phoon and Kulhway (1999) reported suggested guidelines of SOF for a
205 range of soil properties (e.g. undrained shear strength, cone tip resistance, water content,
206 effective unit weight, etc.) based on a comprehensive review of various test
207 measurements and it was found that the vertical SOF generally ranges between 0.1 and
208 12.7 m, while the horizontal SOF typically ranges between 3 and 80 m. Several other
209 researchers (Lacasse and Lamballerie, 1995; Vanmarcke, 1977) also found similar
210 ranges of vertical and horizontal scales of fluctuation to those reported by Phoon and
211 Kulhway (1999) for the cone penetration resistance of sand and clay. However, to the
212 authors' best knowledge, no records have been published in relation to SOF of c_h . It is
213 believed that SOF of c_h should be within a range similar to that of other soil properties
214 reported in the literature. This is due to the fact that spatial correlation structure of a soil
215 mass is caused by changes in the constitutive nature of soil over the ground; therefore,
216 c_h would have similar scales of fluctuation to other soil properties.

217

218 In order to model the spatial randomness of c_h , a probability distribution function of its
219 variation should be used and a number of different probability distributions for c_h have
220 been suggested in the literature. For example, Chang (1985) and Hong (1992) used

221 both lognormal and gamma distributions, and a study carried out by Zhou et al. (1999)
 222 considered the Weibull distribution together with the lognormal and gamma
 223 distributions. However, in the current study, the variability of c_h is characterized by a
 224 lognormal distribution because the observation from field tests data reported by Chang
 225 (1985) suggested that the variation of c_h can be adequately modeled by a lognormal
 226 distribution. In addition, the lognormal distribution offers mathematical convenience
 227 because of having simple relationship with the normal distribution. The probability
 228 density function of the assumed lognormally distributed c_h with a mean, μ_{c_h} , and
 229 standard deviation, σ_{c_h} , can thus be given by:

230

$$231 \quad f(c_h) = \frac{1}{c_h \sigma_{\ln c_h} \sqrt{2\pi}} \exp \left[-\frac{1}{2} \left(\frac{\ln c_h - \mu_{\ln c_h}}{\sigma_{\ln c_h}} \right)^2 \right] \quad (1)$$

232

233 where: $\mu_{\ln c_h}$ and $\sigma_{\ln c_h}$ are, respectively, the mean and standard deviation of the
 234 underlying normally distributed c_h , i.e. $\ln(c_h)$, obtained from the specified μ_{c_h} and σ_{c_h}
 235 of the lognormally distributed c_h using the following transformation functions (Fenton
 236 and Griffiths, 2008):

237

$$238 \quad \mu_{\ln c_h} = \ln \mu_{c_h} - \frac{1}{2} \sigma_{\ln c_h}^2 \quad (2)$$

239

240 and

241

$$242 \quad \sigma_{\ln c_h} = \sqrt{\ln\left(1 + \frac{\sigma_{c_h}^2}{\mu_{c_h}^2}\right)} = \sqrt{\ln(1 + v_{c_h}^2)} \quad (3)$$

243

244 where: $v_{c_h} = \sigma_{c_h} / \mu_{c_h}$ is the coefficient of variation of horizontal coefficient of
 245 consolidation. Therefore, in order to properly acknowledge and quantify the spatial
 246 variability of c_h , the following spatial variability characteristics of c_h need to be
 247 identified: the mean, μ_{c_h} , standard deviation, σ_{c_h} , and correlation length, θ_{c_h} .

248

249 In order to determine the above statistical characteristics of c_h for a certain site, a
 250 carefully-controlled geotechnical site investigation program of closely-spaced soil
 251 boring and testing needs to be undertaken, and obtained data be analyzed. However,
 252 such a comprehensive site investigation program is often beyond the scope of most
 253 projects and in the absence of such field information, traditional site investigation of
 254 limited soil testing together with information from the geological maps and knowledge
 255 from previous site investigation of nearby locations can be used to assign reasonable
 256 level of soil variability for the site in question. In addition, the typical ranges of
 257 statistical parameters of c_h available in the literature (Beacher and Christian, 2003) can
 258 be used to assign reasonable values of soil variability of c_h , provided that they are
 259 extracted from similar geologic origins and collected over limited spatial extents.
 260 Detailed description of methods that can be used for evaluating the spatial variation of
 261 soil properties is beyond the scope of the present paper and can be found in many
 262 publications (e.g. DeGroot and Baecher, 1993; Jaksa et al., 1997; Phoon and Kulhawy,
 263 1999; Vanmarcke, 1984).

264

265 **Development of analytical formulation for design factors**

266

267 As indicated earlier, soil consolidation by PVDs takes place by simultaneous vertical
268 and horizontal (radial) drainage of water. The analytical solution for the degree of
269 consolidation due to the horizontal drainage $U_h(t)$, is given by Hansbo (1981) as follows
270 (see Fig. 1 for demonstration of parameters):

271

$$272 \quad U_h(t) = 1 - \exp\left(-\frac{2c_h t}{r_e^2 \alpha}\right) \quad (4)$$

273

274 and

275

$$276 \quad \alpha = F_n + F_s + F_r \quad (5)$$

277

278 where: F_n , F_s and F_r are the drain spacing, smear and well-resistance factors,
279 respectively, which can be expressed as follows:

280

$$281 \quad F_n = \frac{n^2}{(n^2 - 1)} \left[\ln(n) - \frac{3}{4} + \frac{1}{n^2} - \frac{1}{4n^2} \right] \approx \ln(n) - \frac{3}{4} \quad (6)$$

282

$$283 \quad F_s = \left(\frac{k_h}{k'_h} - 1 \right) \ln\left(\frac{r_s}{r_w} \right) = \left(\frac{k_h}{k'_h} - 1 \right) \ln(s) \quad (7)$$

284

$$285 \quad F_r = \frac{2\pi L^2 k_h}{3 q_w} \quad (8)$$

286 where: c_h is the coefficient of consolidation in the horizontal direction; r_e is the radius of
 287 equivalent soil cylinder with impermeable perimeter or the radius of zone of influence; t
 288 is the consolidation time; α is a group parameter representing the smear effects and
 289 geometry of the PVD system; $n = r_e/r_w$ is the drain spacing ratio (r_w is the equivalent
 290 radius of the drain); $s = r_s/r_w$ is the smear ratio (r_s is the radius of the smear zone); k'_h is
 291 the horizontal permeability in the smear zone; L is the maximum vertical drainage
 292 distance; and q_w is the vertical discharge capacity of the drains. If the effects of both the
 293 horizontal and vertical drainage are considered, the analytical solution for the overall
 294 degree of consolidation, $U(t)$, can be obtained as follows (Carillo, 1942):

295

$$296 \quad U(t) = 1 - [1 - U_v(t)][1 - U_h(t)] \quad (9)$$

297

298 where: $U_v(t)$ is the degree of consolidation due to vertical drainage at any time t , that
 299 can be determined as follows (Lambe and Whitman, 1969):

300

$$301 \quad U_v(t) = 1 - \sum_{i=0}^{\infty} \frac{2}{M^2} \exp\left(-M^2 \frac{c_v t}{L^2}\right) \quad (10)$$

302

303 where: $M = \pi/2(2i+1)$; c_v is the coefficient of consolidation in the vertical direction.

304

305 The design of PVD systems using the analytical solutions set out above has been
 306 traditionally carried out deterministically by assuming that the consolidating soil mass
 307 surrounding the PVDs is homogeneous (i.e. soil variability is ignored) with constant
 308 mean values of soil properties across the soil mass. In such case, the drain spacing, S , or

309 the radius of influence zone, r_e , can be determined by iteratively solving Eq. (11) which
 310 is derived by substituting Eq. (4) into Eq. (9), as follows:

311

$$312 \quad r_e^2 \alpha(r_e) = \frac{2t_s \mu_{c_h}}{\ln\left(\frac{1-U_v(t_s)}{1-U_s(t_s)}\right)} \quad (11)$$

313

314 It should be noted that the term $\alpha(r_e)$ in Eq. (11) represents α given in Eq. (4) but used
 315 herein to highlight the fact that the factor α is a function of r_e .

316

317 As c_h is spatially variable, using the deterministically estimated value of r_e as described
 318 above, the degree of consolidation achieved at time t_s may not satisfy the target degree
 319 of consolidation $U_s(t_s)$, resulting in the entire ground improvement process to be
 320 unsuccessful. In order to take into account the spatial variability of c_h , r_e or S is
 321 computed from the proposed probabilistic approach. The approach involves
 322 determination of a factored c_h (i.e. c_{hf}) in such a way that the probability of $U(t_s) \geq$
 323 $U_s(t_s)$, i.e. $P[U(t_s) \geq U_s(t_s)]$, is equal to the specified target probability of achieving
 324 certain degree of consolidation, P_s , in which $P_s = P[U(t_s) \geq U_s(t_s)]$. In other words, if c_{hf}
 325 is used in computing the spacing of PVD, the target degree of consolidation $U_s(t_s)$ can
 326 be achieved at P_s . The factored c_{hf} can then be expressed in the form of the design
 327 factor, D_f , times the mean value of the horizontal coefficient of consolidation, μ_{c_h} , i.e.
 328 $c_{hf} = D_f \mu_{c_h}$. Since $U(t)$ is a monotonically increasing function of c_h , the following
 329 relationship holds (Benjamin and Cornell, 1970; Zhou et al., 1999):

330

331 $P_s = P[U(t_s) \geq U_s(t_s)] = P[c_h \geq c_{hf}]$ (12)

332

333 where: $P[\bullet]$ = probability of its argument.

334

335 It has mentioned earlier that the probability distribution of c_h is assumed to be
 336 lognormally distributed. Therefore, Eq. (12) can be rewritten in the form of the
 337 following lognormal probability distribution transformation:

338

339 $P_s = P[c_h \geq c_{hf}] = 1 - \Phi\left(\frac{\ln c_{hf} - \mu_{\ln \bar{c}_h}}{\sigma_{\ln \bar{c}_h}}\right)$ (13)

340

341 where: $\Phi(\bullet)$ is the standard normal cumulative distribution function; $\mu_{\ln \bar{c}_h}$ and $\sigma_{\ln \bar{c}_h}$ are
 342 respectively, the locally averaged mean and standard deviation of the underlying
 343 normally distributed c_h . In order to obtain c_{hf} from Eq. (13) for a given P_s , $\mu_{\ln \bar{c}_h}$ and
 344 $\sigma_{\ln \bar{c}_h}$ must be obtained by expressing them in terms of the known statistical input
 345 parameters of c_h (i.e. μ_{c_h} , σ_{c_h} and θ_{c_h}). Before finding $\mu_{\ln \bar{c}_h}$ and $\sigma_{\ln \bar{c}_h}$, a brief
 346 discussion in regards to these two parameters is essential and presented below. It should
 347 be noted that the basis of using the locally averaged soil properties to incorporate spatial
 348 variations of soil was first introduced by Fenton and Griffiths (2008), who successfully
 349 used this concept in some applications in geotechnical engineering (e.g. design of
 350 shallow foundations) which was found to give compatible results to those obtained from
 351 the finite element Monte Carlo solutions.

352

353 The enormous significance of spatial variability to soil consolidation is that during the
354 consolidation process water must escape and during the escape process the water must
355 circumnavigate low permeability areas in favor of high permeability areas. In other
356 words, in a consolidating heterogeneous soil mass, high flow rates in some regions of
357 high k_h are offset by lower flow rates in other regions of low k_h , meaning that the total
358 flow from the vicinity of PVD is effectively an averaging process. This is to say that the
359 overall behavior of PVD system is not governed by the soil properties at discrete points
360 but by the average soil properties of the soil volume within the soil domain. It should be
361 noted that, the random fields are characterized by their point statistics, meaning that
362 μ_{c_h} , σ_{c_h} and θ_{c_h} of c_h are defined at the point level. However, soil properties are rarely
363 measured at a point and most engineering measurements concerned with soil properties
364 are performed on samples of some finite volume. Therefore, the measured soil
365 properties are actually locally averaged over the sample volume. For example, the
366 permeability of soil is generally estimated using a laboratory sample of some volume
367 which involves measuring the amount of water which passes through the sample in
368 some time interval. The paths that the water takes to escape from the sample are not
369 considered individually; rather all the flow paths are taken into account together. It
370 should be note that the permeability of soil at the point level is either infinite (in case of
371 a void) or zero (in case of solid). In the light of this, the flow of water through the
372 spatially variable soil into the drain is essentially a process governed by the locally
373 averaged soil properties (Fenton and Griffiths, 2008). The main effects of the local
374 averaging are to reduce the point variance and damp the contribution from the high
375 frequency components. If the point distribution of the soil property of interest is
376 normally distributed, the local averaging process will lead to a reduction in the point

377 variance but the mean will not be affected. For the lognormal distribution, however,
 378 both the mean and standard deviation will be reduced by the local averaging. This is
 379 because the mean of a lognormal distribution depends on both the mean and variance of
 380 the underlying normal distribution. Based on the above discussion, the locally averaged
 381 mean of the underlying normally distributed c_h (i.e. $\mu_{\ln \bar{c}_h}$) is unaltered by the local
 382 averaging and can be given by:

$$384 \quad \mu_{\ln \bar{c}_h} = \mu_{\ln c_h} \tag{14}$$

385
 386 Using Eqs. (2) and (3), $\mu_{\ln \bar{c}_h}$ can be expressed in terms of the known point statistics of
 387 c_h , as follows:

$$389 \quad \mu_{\ln \bar{c}_h} = \mu_{\ln c_h} = \ln \mu_{c_h} - \frac{1}{2} \ln(1 + \nu_{c_h}^2) \tag{15}$$

390
 391 According to the local averaging theory (Vanmarcke, 1984), the locally averaged
 392 standard deviation of the underlying normally distributed c_h (i.e. $\sigma_{\ln \bar{c}_h}$) can be given by:

$$394 \quad \sigma_{\ln \bar{c}_h} = \sigma_{\ln c_h} \sqrt{\gamma(D)} \tag{16}$$

395
 396 where: $\gamma(D)$ is the “variance reduction function” that defines the amount by which the
 397 point variance is reduced as a result of the local averaging over the domain D and is a

398 function of the size of the averaging domain and scale of fluctuation. Using Eq. (3),
 399 $\sigma_{\ln \bar{c}_h}$ in Eq. (16) can be expressed in terms of specified point statistics of c_h , as follows:

400

$$401 \quad \sigma_{\ln \bar{c}_h} = \sqrt{\gamma(D) \ln(1 + \nu_{c_h}^2)} \quad (17)$$

402

403 Using Eqs. (15) and (17), and replacing c_{hf} by $D_f \mu_{c_h}$, Eq. (13) gives:

404

$$405 \quad P_s = P[c_h \geq c_{hf}] = 1 - \Phi \left(\frac{\ln D_f + \frac{1}{2} \ln(1 + \nu_{c_h}^2)}{\sqrt{\gamma(D) \ln(1 + \nu_{c_h}^2)}} \right) \quad (18)$$

406

407 Eq. (18) can now be rewritten as follows:

408

$$409 \quad D_f = \frac{1}{\sqrt{1 + \nu_{c_h}^2}} \exp \left[\Phi^{-1}(1 - P_s) \sqrt{\gamma(D) \ln(1 + \nu_{c_h}^2)} \right] \quad (19)$$

410

411 where: $\Phi^{-1}(\bullet)$ is the inverse normal cumulative distribution function.

412 If sufficient data at the site is available, the mean and variance of the soil property of
 413 interest can be established with reasonable confidence. However, unlike the mean and
 414 variance, reasonable estimation of the statistics regarding the spatial correlation
 415 structure is not utterly straightforward. In the following section, the procedure for
 416 obtaining the correlation structure of soil is described and discussed.

417

418

419 **Estimation of correlation structure of soil**

420

421 As mentioned earlier, soil properties measured at two spatial locations may be
422 correlated or uncorrelated depending on the correlation structure of a soil. The concept
423 of spatial correlation between soil properties at two disjoint points can be captured
424 mathematically using the theoretical correlation function, which is generally fitted to the
425 sample correlation function (obtained from measured data) to determine the scale of
426 fluctuation. The sample correlation function, $\rho(\tau)$, is the plots of sample correlation
427 against separation or lag distances, τ . To obtain this, the sample covariance, $\text{Cov}[X_i,$
428 $X_{i+\tau}]$, is generally normalized by the sample variance, $\text{Var}[X]$, as follows:

429

430
$$\rho(\tau) = \frac{\text{Cov}[X_i, X_{i+\tau}]}{\text{Var}[X]} \quad (20)$$

431

432 where: X represents a spatially variable soil property.

433

434 The computed sample correlation function is then fitted with an assumed theoretical
435 correlation function to determine the scale of fluctuation, θ . A number of theoretical
436 correlation functions are indicated in the literature (e.g. Fenton and Griffiths, 2008;
437 Vanmarcke, 1977) to represent the correlation of a soil property in the ground. Upon
438 deciding on the theoretical correlation function that represents the correlation structure
439 of the soil property in question, the variance reduction factor can be estimated from the
440 corresponding variance function of the selected correlation structure. In the following
441 section, a simplified procedure for obtaining the variance reduction factor is described
442 and discussed.

443 **Approximation to the variance reduction factor**

444

445 Since Eq. (4) only accounts for soil consolidation due to radial drainage from a
446 horizontal plane passes through the vertical drain, c_h can be considered as 2D random
447 field. This means that on a horizontal (x - y) plane, c_h is spatially variable and in the
448 vertical (z) direction it is spatially constant. In other words, θ_{c_h} is finite in x and y
449 directions, and infinite (∞) in z direction. The spatial correlation structure of c_h is also
450 assumed to be statistically isotropic, i.e. the scales of fluctuation in the x and y
451 directions on a horizontal plane are assumed to be the same (i.e. $\theta_{c_h(x)} = \theta_{c_h(y)} = \theta_{c_h}$).
452 Although the correlation structures in any spatial direction are usually different, the
453 reason for assuming c_h as an isotropic random field is that the correlation structure is
454 more related to the formation process (i.e. layer deposition). Therefore, on a horizontal
455 plane the spatial correlation structure of c_h would have similar scales of fluctuation in
456 any direction. In addition, the scale of fluctuation is a difficult parameter to estimate in
457 practice and assuming an isotropic condition with smaller scale of fluctuation will
458 provide slightly conservative results (Fenton and Griffiths 2008). Based on the above
459 discussion, the correlation structure of c_h is idealized by applying an isotropic two-
460 dimensional (2D) exponentially decaying (Markovian) spatial correlation function of
461 the following form:

462

463
$$\rho_{\ln c_h}(\tau) = \exp\left(-\frac{2|\tau|}{\theta_{c_h}}\right) \quad (21)$$

464

465 where: $|\tau| = \sqrt{\tau_x^2 + \tau_y^2}$ is the absolute distance between two points in the soil domain (τ_x
 466 and τ_y are, respectively, the difference between the x and y coordinates of any two points
 467 in the random field). Although any correlation function can be employed, the Markov
 468 correlation function is selected because of its simplicity and ease of implementation.

469

470 Now the variance reduction factor can be estimated from the corresponding variance
 471 function of the 2D Markov correlation function shown in Eq. (21), as follows:

472

$$473 \quad \gamma(D) = \gamma(X, Y) = \frac{1}{X^2 Y^2} \times \int_0^X \int_0^X \int_0^Y \int_0^Y \rho(\zeta_1 - \eta_1, \zeta_2 - \eta_2) d\zeta_1 d\eta_1 d\zeta_2 d\eta_2 \quad (22)$$

474

475 where: X and Y are the dimensions of the averaging domain in the x and y directions,
 476 respectively (i.e. $D = X \times Y$). As mentioned earlier, the variance reduction factor is a
 477 function of the size of the averaging domain and scale of fluctuation. Numerical
 478 integration of the function shown in Eq. (22) leads to the variance reduction factor that
 479 varies between 0 and 1, depending on the values of S (or r_e) and θ_{c_h} . The detailed
 480 calculation procedure of the variance reduction factor is given in Appendix A.

481

482 ***Development of chart for the variance reduction factor***

483

484 Using the algorithm shown in Appendix A, a chart for the variance reduction factor
 485 estimated over a wide range of S and θ_{c_h} that are likely to be encountered in reality is
 486 presented in Fig. 2. As in practice, PVDs are installed with a drain spacing of 1–3 m
 487 (Walker, 2011), thus, the variance reduction factor is estimated over S ranges between

488 1–3 m. Theoretically, θ_{c_h} can have values ranging from zero to infinity, when θ_{c_h} tends
489 to be zero $\gamma(D)$ also tends to be zero, whereas when θ_{c_h} to be infinity $\gamma(D)$ tends to be
490 unity. Therefore, the minimum and maximum values of θ_{c_h} are chosen so as to cover all
491 the values of $\gamma(D)$ from 0 to 1. It should be noted that, for the interest of generality, θ_{c_h}
492 in Fig. 2 is expressed in the non-dimensional form Θ ($\Theta = \theta_{c_h} / S$). It should also be
493 noted that, in practice, PVDs are installed in a square or triangular pattern, thus, the
494 geometry of the influence area of each drain is either square (for square pattern
495 installation) or hexagonal (for triangular pattern installation) depending on the
496 installation pattern. The influence area of an individual PVD can also be represented by
497 an equivalent circular area for both installation patterns. However, a closed form
498 solution for the variance function does not exist for most of the correlation function in
499 two or higher dimensions. In such case, it can be obtained by numerical integration (see
500 Eq. (22)). Therefore, to avoid superfluous complexity in the numerical integration, $\gamma(D)$
501 plotted in Fig. 2 is approximated based on an equivalent square influence area of side
502 length S irrespective of the installation fashion.

503

504 **Development of probabilistic design procedure and charts**

505

506 As can be seen in Eq. (19), for a given P_s and ν_{c_h} , D_f can be expressed as a function of
507 $\gamma(D)$. The calculated values of D_f over the range of $\gamma(D)$ for different values of P_s and
508 ν_{c_h} are presented in Fig. 3. It can be seen from each individual figure that for any
509 certain ν_{c_h} , D_f is a decreasing function of P_s and $\gamma(D)$. What this means is that a lower
510 value of c_h is required if the specified reliability of achieving a target degree of

511 consolidation is high. Comparison between Figs. 3a–e reveals that for a certain P_s and
 512 $\gamma(D)$, D_f is also a decreasing function of ν_{c_h} . In other words, if the uncertainty of c_h
 513 increases, smaller value of c_h is required.

514

515 Using the appropriate value of D_f based on the prescribed values of P_s , ν_{c_h} and $\gamma(D)$ can
 516 be obtained from the chart shown in Fig. 3 and the design of soil consolidation via
 517 PVDs can be carried out in a similar way to that described by Zhou et al. (1999). The
 518 design process involves estimation of the drain spacing, S , to satisfy a target degree of
 519 consolidation, $U_s(t_s)$. In order to determine S , the required values of r_e (i.e. r_{es}) using the
 520 design values of c_h (i.e. c_{hf}) need to be calculated first. Then S can be obtained from the
 521 calculated r_{es} using the available conversion formulae. It should be noted that for the
 522 rectangular pattern installation $S = r_{es}/0.565$, while $S = r_{es}/0.525$ for the triangular
 523 pattern.

524

525 By replacing c_h with its design factored value c_{hf} in Eq. (11) and dividing both sides of
 526 Eq. (11) by r_w^2 , the following equation yields:

527

$$528 \left(\frac{r_{es}}{r_w} \right)^2 \alpha(r_{es}) = \frac{2t_s D_f \mu_{c_h}}{\ln \left(\frac{1 - U_v(t_s)}{1 - U_s(t_s)} \right)} \frac{1}{r_w^2} \quad (23)$$

529

530 Eq. (23) can be expressed in a graphical form for different values of $F_s + F_r$ as shown
 531 in Fig. 4 where the horizontal and the vertical axes are defined by:

532

$$533 \quad \psi = \frac{2t_s D_f \mu_{c_h}}{\ln\left(\frac{1-U_v(t_s)}{1-U_s(t_s)}\right)} \frac{1}{r_w^2} \quad (24)$$

534

535 and $n = r_e/r_w$, respectively. Now Figs. 3 and 4 can be used for design of ground

536 improvement by PVDs using the following steps:

- 537 1. Select an appropriate PVD on the basis of discharge capacity, q_w , jacket filter
538 characteristics, material strength and durability, and calculate its equivalent drain
539 radius $r_w = (a + b)/\pi$, where: a and b are the width and thickness of the PVD,
540 respectively;
- 541 2. Determine the characteristic values of all other deterministic parameters involved in
542 the design including c_v , k_h , and L and estimate k'_h and r_s based on the installation
543 procedure, mandrel size, and shape and soil micro fabric then calculate r_s/r_w , k_h/q_w
544 and k_h/k'_h ;
- 545 3. Find the mean, standard deviation and scale of fluctuation of c_h , i.e. μ_{c_h} , σ_{c_h} and
546 θ_{c_h} ; and calculate $\nu_{c_h} = \sigma_{c_h} / \mu_{c_h}$;
- 547 4. Specify certain consolidation time, t_s , and corresponding degree of consolidation,
548 $U_s(t_s)$;
- 549 5. Calculate $U_v(t_s)$ using Eq. (10);
- 550 6. Assume an initial drain spacing, S_a , for the probabilistic design and using S_a and
551 θ_{c_h} find the variance reduction factor, $\gamma(D)$ via chart provided in Fig. 2 if there is
552 any lack of improved site information;

- 553 7. For a given probability of achieving the target degree of consolidation, P_s ,
554 determine the design factor D_f from Fig. 3 and if v_{c_h} is such that it stands between
555 two consecutive figures in Fig. 3, use linear interpolation to determine an
556 appropriate D_f ;
- 557 8. Calculate ψ from Eq. (24) and $F_s + F_r$ using Eqs. (7) and (8);
- 558 9. Find the value of n from Fig. 4 using the values of ψ and $F_s + F_r$ obtained in Step 8,
559 and calculate $r_{es} = nr_w$;
- 560 10. Obtain the design drain spacing, S , using $S = r_{es}/0.565$ for the rectangular pattern or
561 $S = r_{es}/0.525$ for the triangular pattern;
- 562 11. If the calculated S in Step 11 is equal to the initially assumed S_a in Step 6, then the
563 design process ends; otherwise repeat Steps 6–11 until $S \approx S_a$.

564 It can be noticed that the probabilistic design procedure set out above is iterative and
565 this is due to the fact that $\gamma(D)$, which is required for the determination of D_f , is a
566 function of the design parameter S . Therefore, to reduce the number of iteration for
567 obtaining S , it is instructive to proceed with the deterministic design by setting the
568 design factor D_f equal to unity in Eq. (23). The deterministically designed drain spacing,
569 S_D , or a slightly lower value of S_D (e.g. 25% smaller than S_D) can be used as S_a for the
570 first iteration. Following this procedure, the required number of iteration may be
571 reduced to be 3 or 4 iterations. It is noteworthy mentioning that the solution proposed
572 by Hong and Shang (1998) and Zhou et al. (1999) is a special case of the PDM
573 presented in this work. If D_f is obtained from Fig. 3 by setting $\gamma(D) = 1$, it will give the
574 same solution as that of the design procedure presented by Hong and Shang (1998) and
575 Zhou et al. (1999). Therefore, the design procedure of Hong and Shang (1998) and
576 Zhou et al. (1999) is applicable for soil variability only when c_h within the influence

577 zone becomes perfectly correlated (i.e. when $\theta_{c_h} \rightarrow \infty$). To further facilitate the use of
578 the proposed PDM, an executable computer program suitable for use by practitioners is
579 developed and can be provided upon request.

580

581 **Stochastic Finite Element Monte Carlo Approach**

582

583 To demonstrate the validity of the proposed PDM, a series of stochastic FEMC analyses
584 are performed and used for comparison with the PDM. The stochastic FEMC approach
585 merges the local average subdivision (LAS) method (to generate random c_h fields) and
586 finite element modeling (to calculate soil consolidation by PVDs) into a Monte Carlo
587 framework using the following steps:

- 588 1. Create a virtual soil profile for specified site conditions which comprises a grid of
589 elements allowing arbitrary distributions of coefficient of consolidation to be
590 modeled across the grid. This is achieved by generating spatially variable random
591 coefficient of consolidation field using the local average subdivision (LAS) method
592 developed by Fenton and Vanmarcke (1990);
- 593 2. Incorporate the generated spatial variability of the coefficient of consolidation into
594 the finite element modeling of soil consolidation by PVDs; and
- 595 3. Repeat Steps 1 and 2 many times using the Monte Carlo technique so that a series of
596 consolidation responses can be obtained from which the probability of achieving a
597 target degree of consolidation at a specified time can be estimated.

598 As the geometry and drain spacing of the problem at hand need to be known for the
599 finite element analysis, the consolidation problem under consideration with given $U_s(t_s)$,

600 P_s , t_s , ν_{c_h} and θ_{c_h} is designed first by the PDM. The above steps are then applied to a
601 consolidation problem of a known geometry. Within the scope of the paper the above
602 steps are briefly described in the following sections, and detailed description of the
603 steps used can be found in Shahin and Bari (2012).

604

605 ***Generation of spatially variable horizontal coefficient of consolidation*** 606 ***field***

607

608 It has already mentioned earlier that c_h is considered as the only random variable in the
609 proposed PDM and can be reasonably idealized as a 2D random field. Accordingly, by
610 employing the specified values of μ_{c_h} , σ_{c_h} and θ_{c_h} , 2D random field of c_h is generated
611 using the LAS method (Fenton and Vanmarcke, 1990). The LAS algorithm generates c_h
612 field in the form of a grid of cells that are assigned locally averaged values of c_h
613 different from one another across the grid, albeit remain constant within each element of
614 the soil domain (c_h is generally measured using some representative volume, the
615 constant value of c_h within each element is deemed to be such measure). Using the LAS
616 code, random field of c_h is generated in such a way that the number of grid cells is equal
617 to the number of the finite elements of the soil mass, taking full account of the finite
618 element size in the local averaging process.

619

620 In the process of simulating random field of c_h , correlated local averages of standard
621 normal random field $G(x)$ are first generated with zero mean, unit variance and spatial
622 correlation function using the LAS technique. The correlation coefficient between c_h
623 measured at a point x_1 and a second point x_2 is specified by the correlation function

624 shown previously in Eq. (21). As c_h is assumed to be characterized statistically by a
625 lognormal distribution, the correlated standard normal random field, $G(x)$, generated by
626 the LAS method is then transformed into a lognormal distribution using the following
627 transformation function (Fenton and Griffiths, 2008):

$$629 \quad c_{h_i} = \exp\{\mu_{\ln c_h} + \sigma_{\ln c_h} G(x_i)\} \quad (25)$$

630
631 where: x_i and k_i are, respectively, the vector containing the coordinates of the center of
632 the i th element and the soil property value assigned to that element. It should be noted
633 that the random fields of c_h are generated using the free available 2D LAS computer
634 code (<http://www.engmath.dal.ca/rfem/>) implying that θ_{c_h} in the vertical direction (z -
635 direction) is infinite (i.e. the soil properties in this direction remain constant).

636

637 ***Finite element modeling incorporating spatial variability of horizontal***
638 ***coefficient of consolidation***

639

640 With the complete subsurface profile having been simulated in the previous step, the
641 spatial variability of c_h is now known and can be employed as input in a finite element
642 consolidation modeling of soil improvement by PVDs. All numerical analyses are
643 carried out using a modified version of the finite element computer program “p86”
644 from the book by Smith and Griffiths (2004) in which soil consolidation is treated as a
645 2D uncoupled problem under axisymmetric condition. Originally program “p86” was
646 for general two (plane) or three dimensional analysis of the uncoupled consolidation
647 equation using implicit time integration with the “theta” method. The authors modified

648 the source code of ‘‘p86’’ to allow an axisymmetric and repetitive Monte-Carlo
649 analyses. Although the modified version of ‘‘p86’’ can also be used for 3D analysis, 2D
650 finite element analysis is conducted as 3D FEMC analysis is computationally too
651 intensive. Since only 2D axisymmetric analysis is performed, FE analysis considers
652 only the consolidation due to drainage in the horizontal direction (i.e. consolidation due
653 to drainage in the vertical direction is not estimated from the FE solution). In this study,
654 it is assumed that if the vertical drainage is considered in the FE analysis, it will give
655 the same results as $U_v(t)$, as shown in Eq. (10).

656

657 It can be noticed that the probabilistic design procedures proposed earlier in this paper
658 take the smear effect into account through a constant ratio of permeability in the
659 undisturbed zone to the smear zone (i.e. k_h/k'_h). However, no explicit permeability
660 parameter is considered in the FE analysis. To simulate such reduced permeability
661 condition in the smear zone during the FE analysis, two independent random fields of c_h
662 are generated separately. By employing the specified μ_{c_h} , σ_{c_h} and θ_{c_h} into the LAS
663 method, a random field of c_h is generated first for the whole soil domain and mapped
664 onto the corresponding grid in the finite element mesh. Then another random field of c_h
665 is generated (for the whole influence zone) with modified mean, μ'_{c_h} , and σ'_{c_h} in such a
666 way that $k_h/k'_h = \mu_{c_h} / \mu'_{c_h}$ and $\sigma_{c_h} / \mu_{c_h} = \sigma'_{c_h} / \mu'_{c_h}$ (i.e. same coefficient of variation is
667 employed for both fields). However, for both random fields, the same value of θ_{c_h} is
668 used. Now from the second random field, only the corresponding elements to the smear
669 zone are mapped onto the finite element mesh. This process of random field generation
670 ensures original random nature of c_h over the soil domain and reasonably reflects the

671 smear effect as well. It should be noted that, for simplicity, the well resistance factor
 672 which may affect the rate of consolidation is not considered in the FE analysis. This is
 673 due to the fact that the discharge capacities of most PVDs available in the market are
 674 relatively high, and hence the well resistance effect can be ignored in most practical
 675 cases (Abuel-Naga et al., 2012; Chu, 2004).

676

677 An initial pore water pressure of 100 kPa dissipates in a square domain of side length S
 678 (spacing of PVD system) is considered in all FE analyses. The selection of square
 679 influence area (irrespective of PVD installation pattern) instead of the equivalent
 680 circular influence area is to avoid the unfavourable mesh shape as the LAS method
 681 requires square (or rectangular) elements to accurately compute locally averaged values
 682 of c_h for each element across the grid. For the same reason, square shaped smear zone
 683 of side length $S_s = \sqrt{\pi r_s^2}$ and PVD of side length $S_w = \frac{\pi r_w}{2}$ are employed. A single
 684 generation of a random field and the subsequent finite-element analysis of that field are
 685 termed “realization”. For an individual realization, the degree of consolidation, $U_h(t)$, at
 686 any certain consolidation time, t , is calculated with the help of the following expression:

687

$$688 \quad U_h(t) = 1 - \frac{\bar{u}}{u_0} \quad (26)$$

689

690 where: u_0 = initial pore pressure; and \bar{u} = average pore pressures at any time of the
 691 consolidation process. It has to be emphasized that the average pore pressure (\bar{u}) at any
 692 time of the consolidation process is calculated by numerically integrating the pore
 693 pressure across the volume of each element at a particular time, summing the

694 contribution of each element and dividing by the total mesh area (element areas are also
695 calculated by numerical integration).

696

697 As the accuracy of the finite element analysis is dependent on the mesh density, a
698 sensitivity analysis is carried out for both the deterministic and stochastic solutions on
699 various mesh dimensions to ensure reasonable refinement with minimal discretization
700 error and to produce reliable and reproducible statistics of the output quantities. The
701 consolidation problem under consideration for the mesh sensitivity analysis implies an
702 axisymmetric unit cell of geometry $r_e = 1.467$ m (i.e. $S = 2.6$ m), $r_s = 0.5642$ m (i.e. $S_s =$
703 1 m) and $r_w = 0.1273$ m (i.e. $S_w = 0.2$ m). The mean value of the horizontal coefficient
704 of consolidation for the undisturbed zone, μ_{c_h} , is selected to be equal to $4 \text{ m}^2/\text{year}$. It is
705 assumed that $k_h/k'_h = 2$. To simulate such condition, the mean value of the horizontal
706 coefficient of consolidation for the smear zone, $\mu'_{c_h} = 2 \text{ m}^2/\text{year}$ is used. In order to
707 determine an optimum mesh density, deterministic analysis (using the respective
708 constant mean value of c_h for undisturbed and smear zones) of the above problem is
709 conducted first for three different mesh densities with element size of: $0.2 \text{ m} \times 0.2 \text{ m}$;
710 $0.1 \text{ m} \times 0.1 \text{ m}$; and $0.05 \text{ m} \times 0.05 \text{ m}$. The obtained results are shown in Fig. 5a, which
711 also includes the results of the mesh size analysis for the stochastic analysis (will be
712 described below). It can be seen that the degree of consolidation, U_h , obtained from the
713 mesh size $0.1 \text{ m} \times 0.1 \text{ m}$ is identical to that of the mesh size $0.05 \text{ m} \times 0.05 \text{ m}$, and is
714 marginally different from that of the mesh size $0.2 \text{ m} \times 0.2 \text{ m}$. Accordingly, the mesh
715 size $0.1 \text{ m} \times 0.1 \text{ m}$ is deemed to be suitable for the deterministic analysis. On the other
716 hand, the two mesh sizes: $0.1 \text{ m} \times 0.1 \text{ m}$ and $0.05 \text{ m} \times 0.05 \text{ m}$ are further investigated
717 for the stochastic analysis. After performing a suite of 2000 Monte Carlo simulations

718 for a case study of $\nu_{c_h} = 100\%$ and $\theta_{c_h} = 1.0$, the mean, μ_{U_h} , and standard deviation, σ_{U_h} ,
719 of the degree of consolidation over the 2000 simulations are estimated using the method
720 of moments and the results are shown in Fig. 5. It can be seen that there is little or no
721 change in μ_{U_h} (Fig. 5a) and σ_{U_h} (Fig. 5b) from the mesh size $0.1 \text{ m} \times 0.1 \text{ m}$ to $0.05 \text{ m} \times$
722 0.05 m and thus the mesh size $0.1 \text{ m} \times 0.1 \text{ m}$ is also deemed to give reasonable
723 precision for the stochastic consolidation analysis. However, to comply with the
724 minimum correlation length reported in the literature, it was decided to discretize the
725 soil domain in the current study into the more refined mesh of element size of $0.05 \text{ m} \times$
726 0.05 m .

727

728 ***Repetition of process based on the Monte Carlo technique***

729

730 The accuracy of the estimated statistics of the output quantities of interest is dependent
731 on the number of Monte Carlo simulations. Therefore, to maintain accuracy and run
732 time efficiency, the sensitivity of results to the number of Monte Carlo simulations is
733 examined. The sensitivity analysis indicated that 2000 realizations are sufficient to give
734 reasonably stable output statistics for each analysis of interest. Based on this
735 observation, the process of generating a random field of c_h and the subsequent finite
736 element analysis is repeated 2000 times. Huang et al. (2010) also performed successful
737 probabilistic analysis on soil consolidation using a $0.05 \text{ m} \times 0.05 \text{ m}$ square element
738 mesh with 2000 simulations. At each “realization” of the Monte Carlo process, the
739 random field of c_h is generated using the same ν_{c_h} and θ_{c_h} , but with spatial distribution
740 of c_h that varies from one realization to the next. Fig. 6 shows a typical example of the
741 discretized FE mesh and the corresponding soil domain represented by a grey scale of a

742 typical realization of the random field of c_h in which the magnitude of c_h remains
743 constant within each element but differs from one element to another. The obtained
744 outputs from the suite of 2000 realizations of the Monte Carlo process are collated and
745 statistically analyzed to make a comparative study between the proposed PDM and the
746 FEMC, as will be seen later.

747

748 ***Probabilistic interpretation of the FEMC results***

749

750 In the PDM, the drain spacing S is calculated based on a given $U_s(t_s)$, t_s and P_s , while in
751 the FE analysis S is a known parameter. Therefore, to compare the PDM with the
752 FEMC, the probability of achieving $U_s(t_s)$ (i.e. $P[U \geq U_s]$) at t_s or the probability that t is
753 less than or equal to t_s (i.e. $P[t \leq t_s]$) that achieves $U_s(t_s)$ is to be estimated. In this study,
754 the later process is employed, i.e. $P[t \leq t_s]$ is estimated. This is because determining
755 probability from a set of data requires establishment of a reasonable probability
756 distribution for the data set. However, the obtained fit using the raw data of $U(t_s)$ was
757 typically poor while the distribution of t at $U_s(t_s)$ obtained from the suite of the 2000
758 realizations is reasonably fitted with lognormal distribution and gives sufficiently
759 reasonable approximation to the $P[t \leq t_s]$. By accepting the lognormal distribution for t
760 at any given $U_s(t_s)$, the statistical moments μ_t and σ_t that are representing the mean and
761 standard deviation of the lognormally distributed t are calculated from the suite of 2000
762 realizations using the following transformation functions:

763

$$764 \quad \mu_t = \frac{1}{n_{sim}} \sum_{i=1}^{n_{sim}} t_i \quad (27)$$

765

766
$$\sigma_t = \sqrt{\frac{1}{n_{sim} - 1} \sum_{i=1}^{n_{sim}} [t_i - \mu_t]^2}$$
 (28)

767

768 where: t_i is the t from the i 'th realization ($i = 1, 2, 3, \dots, n_{sim}$) at given $U_s(t_s)$ and n_{sim}
 769 = total number of realizations = 2000. The probability that t is less than or equal to t_s
 770 (i.e. $P[t \leq t_s]$) that achieves $U_s(t_s)$ can then be obtained from the following lognormal
 771 probability distribution transformation:

772

773
$$P[t \leq t_s] = \Phi\left(\frac{\ln t_s - \mu_{\ln t}}{\sigma_{\ln t}}\right)$$
 (29)

774

775 where: $P[.]$ is the probability of its argument; $\Phi(.)$ is the standard normal cumulative
 776 distribution function; $\mu_{\ln t}$ and $\sigma_{\ln t}$ are, respectively, the mean and standard deviation of
 777 the underlying normally distributed $\ln t$ and can be estimated from μ_t and σ_t with
 778 reference to Eqs. (2) and (3), as follows:

779

780
$$\mu_{\ln t} = \ln \mu_t - \frac{1}{2} \sigma_{\ln t}^2$$
 (30)

781

782
$$\sigma_{\ln t} = \sqrt{\ln\left(1 + \frac{\sigma_t^2}{\mu_t^2}\right)}$$
 (31)

783

784

785

786 **Comparison between PDM and FEMC through Illustrative numerical**
787 **example**

788

789 The design methodology described earlier for soil improvement by PVDs is illustrated
790 by the following numerical example. A PVD type is selected with $r_w = 0.06366$ m
791 having a discharge capacity $q_w = 350$ m³/year. The required deterministic parameters are
792 assumed to be: $c_v = 2$ m²/year, $k_h = 1.577 \times 10^{-2}$ m/year, $k'_h = 7.88 \times 10^{-3}$ m/year, $r_s =$
793 0.22568 m, $L = 10$ m. Based on the above parameters, the calculated $r_s/r_w = 3.545$, $k_h/$
794 $k'_h = 2$ and $k_h/q_w = 4.5 \times 10^{-5}$. For the site of interest, it is assumed that $\mu_{c_h} = 4$ m²/ year
795 and $\sigma_{c_h} = 4$ m²/ year. The calculated ν_{c_h} is therefore equal to 100%. It is further
796 assumed that the correlation structure of c_h in any spatial direction can be reasonably
797 represented by the Markov correlation function given in Eq. (21) and the obtained $\theta_{c_h} =$
798 1 m. The design is to be carried out for achieving 90% consolidation, i.e. $U_s(t_s) = 0.90$,
799 with a probability of 95% confidence (i.e. $P_s = 0.95$) after 1 year (i.e. $t_s = 1$ year). The
800 rectangular drain pattern is selected for the drain installation. Following Step 5 of the
801 outlined design procedures, $U_v(t_s)$ is calculated using Eq. (10), which is found to be
802 equal to 0.16.

803

804 It has suggested in the previous section that prior to commencing the probabilistic
805 design, deterministic design would be beneficial from the view point of computational
806 requirement. For deterministic design, the design factor D_f is required to be set equal to
807 unity. Substituting all the parameters calculated earlier in Eq. (24) gives:

808

$$\psi = \frac{2t_s D_f \mu_{c_h}}{\ln\left(\frac{1-U_v(t_s)}{1-U_s(t_s)}\right)} \frac{1}{r_w^2} = \frac{2 \times 1.0 \times 1.0 \times 4.0}{\ln\left(\frac{1-0.16}{1-0.9}\right)} \times \frac{1}{0.06366^2} = 927.4934$$

810

811 As in the finite element analysis, no well resistance effect is considered (i.e. the drain is
812 modeled as a perfect drain), thus $F_r = 0$. Note that, for the selected drain, the estimated
813 well resistance factor using Eq. (8) is very negligible ($F_r = 0.0094$) and the assumption
814 of no well resistance in this case is reasonably accepted. The value of $F_s + F_r$ can then
815 be calculated using Eq. (7) as follows:

816

$$817 \quad F_s + F_r = (2.0 - 1.0) \times \ln(3.545) + 0 = 1.2655$$

818

819 Using the values of ψ and $F_s + F_r$ as calculated above, the value of n reads from Fig. 4
820 as 16.689. Using the value of n in Step 10, the obtained deterministically designed r_e is
821 equal to 1.0624 m (i.e. $16.689 \times 0.06366 = 1.0624$). Since the rectangular pattern is
822 preferred, the corresponding drain spacing, S_D obtained in Step 11 is equal to
823 $1.0624/0.565 = 1.88$ m. Let us now proceed to the probabilistic design.

824

825 **Iteration-1**

826

827 Following Step 6, it is assumed that $S_a = 1.4$ m (25% smaller than S_D). Therefore, $\Theta =$
828 0.714 ($\Theta = \theta_{c_h} / S_a$). The value $\gamma(D)$ corresponding to $\Theta = 0.714$ in Fig. 2 is 0.291.

829 Using $\gamma(D) = 0.291$, $\nu_{c_h} = 100\%$ and $P_s = 0.95$, the value of D_f reads from Fig. 3e as

830 0.3378 . Substituting $D_f = 0.3378$ in Eq. (24) yields:

$$831 \quad \psi = \frac{2t_s D_f \mu_{c_h}}{\ln\left(\frac{1-U_v(t_s)}{1-U_s(t_s)}\right)} \frac{1}{r_w^2} = \frac{2 \times 1.0 \times 0.3378 \times 4.0}{\ln\left(\frac{1-0.16}{1-0.9}\right)} \times \frac{1}{0.06366^2} = 313.33$$

832

$$833 \quad \text{and } F_s + F_r = 1.2655$$

834

835 It should be noted that $F_s + F_r$ is constant for a selected ground improvement problem

836 irrespective of the design approach. By employing the calculated values of ψ and

837 $F_s + F_r$, the value of n reads from Fig. 4 as 10.461. Using the value of n in Step 10, the

838 obtained r_{ep} from the first iteration is equal to 0.6659 m (i.e. $10.461 \times 0.06366 =$

839 0.6659). For the rectangular pattern, the corresponding drain spacing, S , obtained in

840 Step 11 is equal to $0.6659/0.565 = 1.178$ m. As $S \neq S_a$, more iterations are required.

841

842 **Iteration-2**

843

844 Assuming $S_a = 1.18$ m gives $\Theta = 0.8474$ and $\gamma(D) = 0.3436$. Using $\gamma(D) = 0.3436$, the

845 value of D_f reads from Fig. 3e as 0.3168. For $D_f = 0.3168$, $\psi = 293.848$ and

846 $F_s + F_r = 1.2655$. Using these values of ψ and $F_s + F_r$, Fig. 4 yields $n = 10.18$.

847 Therefore, the obtained r_{ep} from the second iteration is equal to 0.648 m. For the

848 rectangular pattern, the corresponding drain spacing, S , obtained in Step 11 is equal to

849 $0.648/0.565 = 1.147$ m. As $S \neq S_a$, proceed to the next iteration.

850

851

852

853 **Iteration-3**

854

855 Assuming $S_a = 1.14$ m gives $\Theta = 0.8772$ and $\gamma(D) = 0.3545$. Using $\gamma(D) = 0.3545$, the
856 value of D_f obtained from Fig. 3e is 0.313. For $D_f = 0.313$, $\psi = 290.212$ and

857 $F_s + F_r = 1.2655$. Using these values of ψ and $F_s + F_r$, Fig. 4 yields $n = 10.127$.

858 Therefore, the obtained r_{ep} from the third iteration is equal to 0.644 m. As the drains are
859 installed in a rectangular fashion, the corresponding drain spacing, S , is equal to 1.14 m.

860 It can be seen that the calculated S is now equal to the initially assumed S_a . Therefore,

861 the designed drain spacing that achieves 90% consolidation with 95% confidence

862 probability ($\nu_{c_h} = 100\%$ and $\theta_{c_h} = 1$ m) is 1.14 m. It is interesting to note that the

863 deterministically designed drain spacing for this problem was 1.88 m.

864 To test the proposed PDM, the FEMC analysis for the above design example is also

865 performed. In the FE analysis, a mesh of square averaging area of side length equal to

866 the drain spacing $S = 1.14$ m as estimated by the PDM is discretized. The same

867 deterministic and random field parameters (i.e. $r_w = 0.06366$ m, $r_s = 0.22568$ m, $r_s/r_w =$

868 3.545 , $\mu_{c_h} = 4$ m²/ year, $\sigma_{c_h} = 4$ m²/ year and $\theta_{c_h} = 1$ m) as that used for the PDM is

869 utilized for the FE analysis. It should be noted that, to simulate $k_h/k'_h = 2$, the random

870 filed for the smear zone (2nd random field) is generated with $\mu'_{c_h} = 2$ m²/ year, $\sigma'_{c_h} = 2$

871 m²/ year and $\theta_{c_h} = 1$ (i.e. ν_{c_h} and θ_{c_h} are kept constant for both random fields). Since

872 soil consolidation due to the vertical drainage is not considered in the FEMC, the time,

873 t , required for achieving $U_h(t_s)$ at each Monte-Carlo simulation is taken as the problem

874 output. It should be noted that, for $U_s(t_s) = 0.90$ and $U_v(t_s) = 0.16$, the calculated $U_h(t_s)$

875 using Eq. (9) is equal to 0.881. In Fig. 7, the legitimacy of the lognormal distribution

876 hypothesis for t is examined by the well-known Chi-square test through frequency
877 density plot of t data at $U_h(t_s) = 0.881$ obtained from the 2000 realizations and a fitted
878 lognormal distribution is superimposed. The visual inspection of Fig. 7 suggests that the
879 lognormal distribution fits the t histogram very well. The goodness-of-fit test using the
880 chi-square test yielded p -value of 0.1 implying that the lognormal distribution
881 hypothesis for t is valid. With reference to Fig. 7, the probability that t is less than or
882 equal to t_s , i.e. $P[t \leq t_s]$, can be estimated as follows:

883

$$884 \quad P[t \leq t_s] = P[t \leq 1] = \Phi\left(\frac{\ln 1 - (-0.82)}{0.46}\right) = 96.3\%$$

885

886 It should be noted that, in case of the PDM, the target probability, P_s , for the problem
887 was 95% implying an excellent agreement between the proposed PDM and the FEMC
888 approaches. Following the same procedure as illustrated above, both the PDM and
889 FEMC are performed over a range of ν_{c_h} and θ_{c_h} as shown in Table 1.

890 The material and geometric properties used for the analyses are shown in Table 2. By
891 specifying $U_s(t_s) = 90\%$, $P_s = 95\%$ and $t_s = 1$ year, the drain spacing S is estimated for
892 each combination of ν_{c_h} and θ_{c_h} using the PDM and listed in Table 3. It can be seen
893 that, for certain ν_{c_h} , the calculated drain spacing S decreases with the increase of θ_{c_h} .

894 The explanation behind this behavior lies in the fact that for a vanishingly small θ_{c_h} ,
895 soil becomes infinitely rough, i.e. any point at which soil has low c_h will be surrounded
896 by points where the soil has high c_h . What this means is that the flow path initially
897 becomes increasingly tortuous with longer drainage length, hence, the flow is forced to
898 find a shorter passage cutting through the low c_h regions. In contrast, for larger θ_{c_h} ,

899 regions of low c_h are bunched together and as a result, the draining pore water detour
900 the bunched up low c_h regions instead of cutting through them which leads to a longer
901 drainage length and consequently slower increasing rate consolidation, subsequently
902 requires a smaller drain spacing.

903

904 The FEMC analysis for each combination of ν_{c_h} and θ_{c_h} is also conducted by
905 employing the estimated S obtained through the PDM. The estimated $P[t \leq t_s]$ at $U_s(t_s) =$
906 90% from the FEMC analysis is displayed in the last row of Table 3 (referred as P_{FEMC}).
907 It can be seen that the target probability P_s (5th row) for the proposed PDM agrees very
908 well with P_{FEMC} (last row). However, the agreement between the proposed PDM and
909 FEMC in Table 3 is examined at a single target probability level, i.e. $P_s = 95\%$.

910 Therefore, to make a general comment regarding the validity of the proposed PDM, it
911 was tested over a wider range of P_s . For this purpose, the same example problem (see
912 Table 2 for the material and geometric properties of the problem) considered earlier to
913 illustrate the design steps of the proposed PDM is used for a design spacing, $S = 1.14$ m
914 (i.e. $r_e = 0.644$ m) and spatial variability parameters of $\nu_{c_h} = 100\%$ and $\theta_{c_h} = 1.0$. Two
915 sets of FEMC analyses are conducted, in the first set, ν_{c_h} is kept constant at 50% for
916 various θ_{c_h} of 0.25 m, 0.5 m and 1.0 m, while in the second set θ_{c_h} is kept constant at
917 1.0 for various ν_{c_h} of 25%, 50% and 100%. It is assumed that $U_s = 90\%$, therefore, the
918 required t of achieving $U_h = 88.1\%$ is targeted at each Monte-Carlo simulation and $P[t \leq$
919 $t_s]$ is calculated as a function of t . The time t to satisfy a certain P_s of achieving $U_s =$
920 90% is determined from the proposed PDM and its results are compared with those
921 obtained from the FEMC. It should be noted that as all geometric properties of the

922 problem is known, $\gamma(D)$ for a certain soil variability is also known. Therefore, using the
 923 known $\gamma(D)$, D_f for a certain P_s can be evaluated from Eq. (19). The calculated D_f can
 924 then be used to obtain t for the PDM using Eq. (23). The results obtained from both the
 925 proposed PDM and FEMC for each set of soil spatial variability parameters mentioned
 926 above are shown in Fig. 8 in which $P[t \leq t_s]$ is expressed as a function of t . It can be
 927 seen that all curves start from the deterministic time of achieving $U_h = 88.1\%$ (i.e.
 928 $t_{D88.1}$). This is due to the fact that $P[t \leq t_s]$ at any time less than the time for the
 929 deterministic target degree of consolidation has little meaning as it implies $D_f > 1.0$
 930 which is physically irrational. For the same reason, a minimum value of $P_s = 70\%$ is
 931 used in developing the chart of D_f shown in Fig. 3.

932

933 The effect of increasing ν_{c_h} on $P[t \leq t_s]$ at a fixed value of $\theta_{c_h} = 1.0$ is illustrated in Fig.
 934 8a, which indicates that the predicted $P[t \leq t_s]$ obtained from the proposed PDM agrees
 935 very well with those obtained from the FEMC for all cases of ν_{c_h} . On the other hand,
 936 Fig. 8b demonstrates that there is also good agreement between $P[t \leq t_s]$ estimated via
 937 the FEMC and proposed PDM, for various values of θ_{c_h} at a fixed value of $\nu_{c_h} = 50\%$,
 938 although a slight discrepancy in $P[t \leq t_s]$ exists when θ is as small as 0.25. As also can
 939 be seen in Table 3, at any certain ν_{c_h} , P_{FEMC} is slightly lower than P_s when θ_{c_h} is too
 940 small (i.e. for erratic soil) implying that the estimated drain spacing using the PDM will
 941 be reasonably un-conservative for very small θ_{c_h} . Close view to the results presented in
 942 Table 3 reveals that P_{FEMC} is higher than P_s when $\theta_{c_h} \geq r_e/2$. What this means is that the
 943 estimated drain spacing using the PDM will be slightly conservative when $\theta_{c_h} \geq r_e/2$.
 944 Since θ_{c_h} is a difficult parameter to estimate in practice, it is suggested to use $\theta_{c_h} \approx r_e$ in

945 the absence of improved site information which will allow slightly conservative
946 estimate of the drain spacing using the PDM.

947

948 It should be noted that although the abovementioned PDM method is mainly developed
949 to consider the inherent soil variability (i.e. aleatoric variability) of c_h , it can also be
950 used to account for the epistemic uncertainty (i.e. measurement error and model
951 uncertainty) of c_h . This can be made by characterizing the probability distribution and
952 COV of c_h , and assuming SOF of c_h to be equal to infinity. The probabilistic design can
953 then be carried out by determining D_f from Fig. 3 corresponding to $\gamma(D) = 1.0$.

954

955 **Conclusions**

956

957 This paper presents a simplified probabilistic design (PDM) method for ground
958 improvement by prefabricated vertical drains (PVDs) taking into account the spatial
959 variability of the horizontal coefficient of consolidation which is deemed to be the most
960 significant random variable affecting soil consolidation. The proposed design approach
961 involves determination of the drain spacing employing a factored design value of the
962 horizontal coefficient of consolidation that achieves a target probability level of specific
963 degree of consolidation at certain timeframe. Simplified design procedure and charts
964 were developed from the proposed probabilistic approach for routine use in practice.

965 The method was verified by a 2D finite element Monte Carlo (FEMC) approach.

966 Although a slight discrepancy between the probabilities of achieving a target degree of
967 consolidation estimated via the PDM and FEMC was observed for very erratic soil (i.e.
968 soil that has very small value of spatial correlation or scale of fluctuation), the overall

969 agreement between this two methods is very good, indicating that the simpler PDM is
970 reliable and can be used with confidence.

971

972

973

974

975

976

977

978

979

980

981

982

983

984

985

986

987

988

989

990

991

992

993 **Notations**

994

c_h	horizontal coefficient of consolidation
c_v	vertical coefficient of consolidation
c_{hf}	factored value of c_h
$\text{Cov}[\dots]$	covariance operator
D_f	design factor
F_n	drain spacing factor
F_r	well-resistance factor
F'_r	average well resistance factor over the entire drain length
F_s	smear factor
k_h	coefficients of permeability in the horizontal (radial) direction
k'_h	horizontal permeability of the smear zone
k_v	coefficients of permeability in the vertical direction
L	maximum vertical drainage distance, length of the vertical drain
m_v	coefficient of volume compressibility
n	drain spacing ratio
q_w	vertical discharge capacity of drains
r_e	radius of the equivalent soil cylinder, radius of the influence zone
r_{es}	required radius of the equivalent soil cylinder for achieving target degree of consolidation
r_w	equivalent radius of the drain
r_s	radius of the smear zone
S	spacing of the drain

S_D	deterministically designed drain spacing
s	smear zone ratio
t	consolidation time
t_s	specified time of consolidation
$U(t)$	degree of consolidation at time t
$U_h(t)$	degree of consolidation due to horizontal drainage at time t
$U_v(t)$	degree of consolidation due to vertical drainage at time t
$U_s(t_s)$	target degree of consolidation at specified time t_s
$U_v(t_s)$	degree of consolidation due to vertical drainage at specified time t_s
v	coefficient of variation of a random variable
v_{c_h}	coefficient of variation of horizontal coefficient of consolidation
γ_w	unit weight of water
α	a group parameter representing the smear effects and geometry of the PVD system
$\gamma(D)$	variance function giving variance reduction due to averaging over domain D
θ	correlation length or scale of fluctuation
θ_{c_h}	scale of fluctuation of horizontal coefficient of consolidation
μ	mean value of a random variable
μ_{c_h}	mean of the lognormally distributed c_h
$\mu_{\ln c_h}$	mean of the underlying normally distributed c_h
$\mu_{\ln \bar{c}_h}$	mean of the logarithm of locally averaged c_h
σ/σ^2	standard deviation/variance of a random variable
σ_{c_h}	standard deviation of the lognormally distributed c_h

$\sigma_{\ln c_h}$	standard deviation of the underlying normally distributed c_h
$\sigma_{\ln \bar{c}_h}$	standard deviation of the logarithm of locally averaged c_h
$\rho_{\ln c_h}(\tau)$	correlation function giving correlation between two $\ln(c_h)$ data separated by a distance τ
τ	absolute distance between two points in the soil domain
P_s	target probability of achieving degree of consolidation
$P(\bullet)$	probability of its argument
$\Phi(\bullet)$	standard normal cumulative distribution function
$\Phi^{-1}(\bullet)$	inverse normal cumulative distribution function

995

996 **Appendix A. Determination of variance reduction factor**

997

998 The amount by which the variance is reduced from the point variance as a result of the
 999 local averaging can be estimated as follows. The fourfold integration in Eq. (22) can be
 1000 condensed to a twofold integration by taking advantage of the quadrant symmetry ($\rho(\tau_1,$
 1001 $\tau_2)=\rho(-\tau_1, \tau_2)=\rho(\tau_1, -\tau_2)=\rho(-\tau_1, -\tau_2)$) of the correlation function in Eq. (21) and can be
 1002 expressed as:

1003

$$1004 \quad \gamma(X, Y) = \frac{4}{X^2 Y^2} \times \int_0^X \int_0^Y (X - \tau_1)(Y - \tau_2) \rho(\tau_1, \tau_2) d\tau_1 d\tau_2 \quad (\text{A.1})$$

1005

1006 Eq. (A.1) can be computed numerically with reasonable accuracy using sixteen-point

1007 Gaussian quadrature integration scheme as follows:

1008

1009
$$\gamma(X, Y) = \frac{1}{4} \sum_{i=1}^{16} \omega_i (1 - \vartheta_i) \sum_{j=1}^{16} \omega_j (1 - \vartheta_j) \rho(\zeta_i, \eta_j) \quad (\text{A.2})$$

1010

1011 where

1012

1013
$$\zeta_i = \frac{X}{2} (1 + \vartheta_i), \eta_j = \frac{Y}{2} (1 + \vartheta_j) \quad (\text{A.3})$$

1014

1015 and

1016

1017 ω_i and ϑ_i , are the weights and Gauss points respectively.

1018

1019

1020

1021

1022

1023

1024

1025

1026

1027

1028

1029

1030

1031

1032

1033 **References**

1034

- 1035 Abuel-Naga, H. M., Pender, M. J., and Bergado, D. T., 2012. Design curves of
1036 prefabricated vertical drains including smear and transition zones effects.
1037 *Geotextiles and Geomembranes*, 32, 1-9.
- 1038 Barron, R. A., 1948. Consolidation of fine-grained soils by drain wells. *Transactions of*
1039 *the American Society of Civil Engineering*, 113, 718-754.
- 1040 Basu, D., Basu, P., and Prezzi, M., 2006. Analytical solutions for consolidation aided by
1041 vertical drains. *Geomechanics and Geoengineering*, 1(1), 63-71.
- 1042 Beacher, G. B., and Christian, J. T., 2003. *Reliability and Statistics in Geotechnical*
1043 *Engineering*, John Wiley & Sons, Chichester, England.
- 1044 Benjamin, J. R., and Cornell, C. A., 1970. *Probability, statistics, and decision for civil*
1045 *engineers*, McGraw-Hill, New York.
- 1046 Bergado, D. T., Alfaro, M. C., and Balasubramaniam, A. S., 1993. Improvement of soft
1047 Bangkok clay using vertical drains. *Geotextile and Geomembranes*, 12(7), 615-
1048 663.
- 1049 Carillo, N., 1942. Simple two- and three-dimensional cases in the theory of
1050 consolidation of soil. *Journal of Mathematics Physicals*, 21(1), 1-5.
- 1051 Chang, C. S., 1985. Uncertainty of one-dimensional consolidation analysis. *Journal of*
1052 *Geotechnical Engineering*, 111(12), 1411-1424.
- 1053 Chu, J., 2004. Practical considerations for using vertical drains in soil improvement
1054 projects. *Geotextiles and Geomembranes*, 22(1), 101-117.

1055 Crawford, C. B., Fannin, R. J., deBoer, L. J., and Kern, C. B., 1992. Experiences with
1056 prefabricated vertical (wick) drains at Vernon, B. C. Canadian Geotechnical
1057 Journal, 29(1), 67-79.

1058 DeGroot, D. J., and Baecher, G. B., 1993. Estimating autocovariance of in-situ soil
1059 properties. Journal of Geotechnical Engineering, 119(1), 147.

1060 Fenton, G. A., and Griffiths, D. V., 2008. Risk assessment in geotechnical engineering,
1061 Wiley, New York.

1062 Fenton, G. A., and Vanmarcke, E. H., 1990. Simulation of random fields via local
1063 average subdivision. Journal of Engineering Mechanics, 116(8), 1733-1749.

1064 Hansbo, S., 1981. Consolidation of fine-grained soils by prefabricated drains.
1065 Proceedings of the 10th International Conference on Soil Mechanics and
1066 Foundation Engineering, Stockholm, Sweden, 677-682.

1067 Hird, C. C., Pyrah, I. C., and Russel, D., 1992. Finite element modelling of vertical
1068 drains beneath embankments on soft ground. Géotechnique, 42(3), 499-511.

1069 Hong, H. P., 1992. One-dimensional consolidation with uncertain properties. Canadian
1070 Geotechnical Journal, 29(1), 161-165.

1071 Hong, H. P., and Shang, J. Q., 1998. Probabilistic analysis of consolidation with
1072 prefabricated vertical drains for soil improvement. Canadian Geotechnical
1073 Journal, 35(4), 666-677.

1074 Huang, J., Griffiths, D. V., and Fenton, G. A., 2010. Probabilistic analysis of coupled
1075 soil consolidation. Journal of Geotechnical and Geoenvironmental Engineering,
1076 136(3), 417-430.

- 1077 Indraratna, B., Rujikiatkamjorn, C., Balasubramaniam, A. S., and McIntosh, G., 2012.
1078 Soft ground improvement via vertical drains and vacuum assisted preloading.
1079 Geotextiles and Geomembranes, 30, 16-23.
- 1080 Jaksa, M. B., Brooker, P. I., and Kaggwa, W. S., 1997. Inaccuracies associated with
1081 estimating random measurement errors. Journal of geotechnical and
1082 geoenvironmental engineering, 123(5), 393-401.
- 1083 Lacasse, S., and Lamballerie, J. Y., 1995. Statistical treatment of CPT data. CPT'95,
1084 Linkoping, Sweden.
- 1085 Lacasse, S., and Nadim, F., 1996. Uncertainties in characterising soil properties.
1086 Proceedings of the Uncertainty in Geologic Environment: From Theory to
1087 Practice, Madison, Wisconsin, 49-75.
- 1088 Lambe, T. W., and Whitman, R. V., 1969. Soil Mechanics, John Wiley & Sons,
1089 Newyork.
- 1090 Lee, I. K., White, W., and Ingles, O. G., 1983. Geotechnical engineering, Pitman,
1091 London.
- 1092 Lumb, P., 1974. Application of statistics in soil mechanics. Soil Mechanics: New
1093 Horizons, London, Newnes-Butterworth, 44-112.
- 1094 Onoue, A., 1988. Consolidation by vertical drains taking well resistance and smear into
1095 consideration. Soils and Foundations, 24(4), 165-174.
- 1096 Phoon, K.-K., and Kulhawy, F. H., 1999. Characterization of geotechnical variability.
1097 Canadian Geotechnical Journal, 36(4), 612-624.
- 1098 Rowe, P. W., 1972. The relevance of soil fabric to site investigation practice.
1099 Géotechnique, 22(2), 195-300.

1100 Rowe, R. K., and Taechakumthorn, C., 2008. Combined effect of PVDs and
1101 reinforcement on embankments over rate-sensitive soils. *Geotextiles and*
1102 *Geomembranes*, 26(3), 239-249.

1103 Shahin, M. A., and Bari, M. W., 2012. Modeling of ground improvement by
1104 prefabricated vertical drains in highly variable soils. *International Conference on*
1105 *Ground Improvement and Ground Control (ICGI 2012)*, University of
1106 Wollongong, Australia, 321-335.

1107 Smith, I. M., and Griffiths, D. V., 2004. *Programming the finite element method*, John
1108 Wiley and Sons.

1109 Terzaghi, K., Peck, R. B., and Mesri, G., 1996. *Soil mechanics in engineering practice*,
1110 Wiley Interscience, New York.

1111 Vanmarcke, E. H., 1977. Probabilistic modelling of soil profiles. *Journal of*
1112 *Geotechnical Engineering Division*, 103(11), 1227-1246.

1113 Vanmarcke, E. H., 1984. *Random fields: analysis and synthesis*, The MIT Press,
1114 Massachusetts.

1115 Walker, R. T., 2011. Vertical drain consolidation analysis in one, two and three
1116 dimensions. *Computers and Geotechnics*, 38(8), 1069-1077.

1117 Walker, R. T., and Indraratna, B., 2006. Vertical drain consolidation with parabolic
1118 distribution of permeability in smear zone. *Journal of Geotechnical and*
1119 *Geoenvironmental Engineering*, 132(7), 937-941.

1120 Yoshikuni, H., and Nakanodo, H., 1974. Consolidation of fine-grained soils by drain
1121 wells with finite permeability. *Soils and Foundations*, 14(2), 35-46.

1122 Zhou, W., Hong, H. P., and Shang, J. Q., 1999. Probabilistic design method of
1123 prefabricated vertical drains for soil improvement. *Journal of Geotechnical and*
1124 *Geoenvironmental Engineering*, 125(8), 659-664.

1125

1126

1127

1128

1129

1130

1131

1132

1133

1134

1135

1136

1137

1138

1139

1140

1141

1142

1143

1144

1145

1146 **Figure Captions:**

1147

1148 **Fig. 1.** Schematic diagram of a unit cell soil cylinder with prefabricated vertical drain

1149 **Fig. 2.** Variance reduction factor as a function of scale of fluctuation

1150 **Fig. 3.** Design factor D_f for (a) $\nu_{c_h} = 10\%$; (b) $\nu_{c_h} = 25\%$; (c) $\nu_{c_h} = 50\%$; (d) $\nu_{c_h} = 75\%$;

1151 (e) $\nu_{c_h} = 100\%$

1152 **Fig. 4.** Design graph for drain spacing [adapted from Zhou et al. (1999)]

1153 **Fig. 5.** Influence of mesh density on (a) U_h (deterministic) and μ_{U_h} (stochastic); (b) σ_{U_h}

1154 **Fig. 6.** Typical realization of the random field c_h with discretized finite element mesh

1155 **Fig. 7.** Frequency density histogram and fitted distribution of t at $U_h = 88.1\%$ for $\nu_{c_h} =$

1156 100% , $\theta_{c_h} = 1.0$

1157 **Fig. 8.** Comparison between FEMC and PDM for the effect of: (a) ν_{c_h} on $P[t \leq t_s]$ for

1158 $\theta_{c_h} = 1.0$ and (b) θ_{c_h} on $P[t \leq t_s]$ for $\nu_{c_h} = 50\%$; at $U_h = 88.1\%$

1159

1160

1161

1162

1163

1164

1165

1166

1167

1168

1169 **Table 1**

1170 Random field parameters for the PDM and FEMC analyses.

Parameter	Value
μ_{c_h} (m ² / year)	4
ν_{c_h} (%)	50, 100
θ_{c_h} (m)	0.25, 0.5, 1.0

1171

1172

1173

1174

1175

1176

1177

1178

1179

1180

1181

1182

1183

1184

1185

1186

1187

1188 **Table 2**

1189 Material and Geometric properties for the PDM and FEMC analyses.

Property	PDM	FEMC
c_v (m ² /year)	2	–
k_h (m/year)	1.577×10^{-2}	–
k'_h (m/year)	7.88×10^{-3}	–
L (m)	10	–
r_w (m)	0.06366	0.06366
r_s (m)	0.22568	0.22568
q_w (m ³ /year)	350	–

1190

1191

1192

1193

1194

1195

1196

1197

1198

1199

1200

1201

1202

1203

1204 **Table 3**

1205 Summary of results obtained from the PDM and FEMC analyses.

Parameter		Value				
$U_s(t_s)$ (%)		90				
t_s (year)		1				
v_{c_h} (%)		50%		100%		
θ_{c_h} (m)	0.25	0.5	1.0	0.25	0.5	1.0
P_s (%)	95	95	95	95	95	95
S (m)	1.69	1.61	1.5	1.44	1.3	1.14
P_{FEMC} (%)	90.9	94.8	96.1	91.7	95.2	96.3

1206

1207

1208

1209

1210

1211

1212

1213

1214

1215

1216

1217

1218

1219

1220

1221

1222

1223

1224

1225

1226

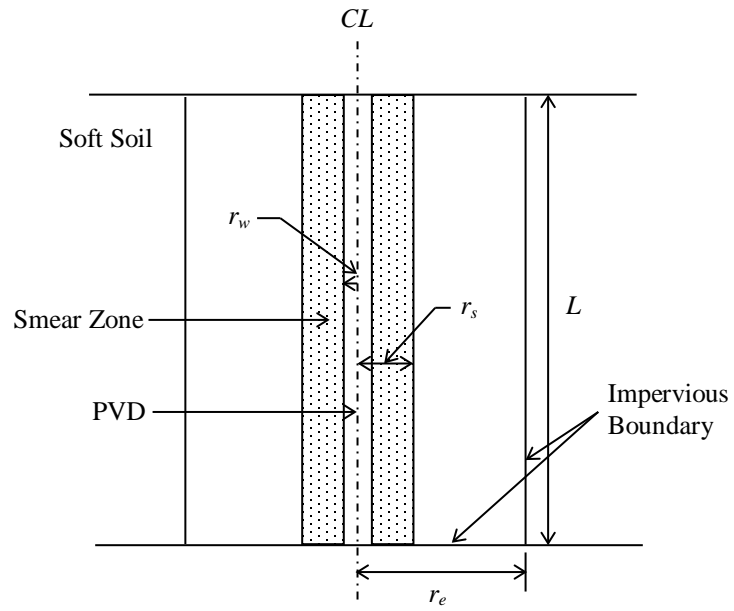
1227

1228

1229

1230

1231



1232

Fig. 1. Schematic diagram of soil cylinder with prefabricated vertical drain

1233

1234

1235

1236

1237

1238

1239

1240

1241

1242

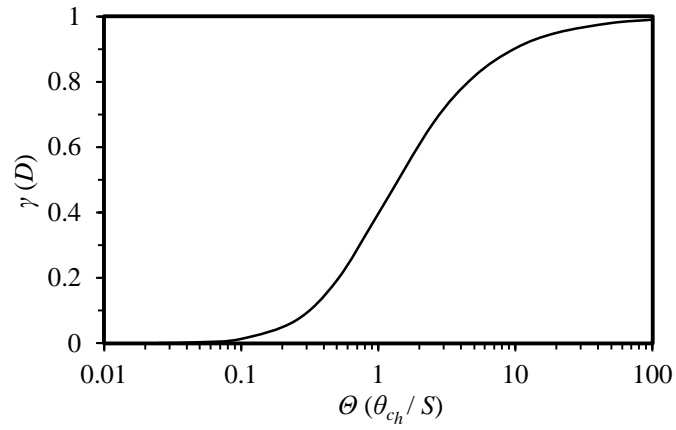
1243

1244

1245

1246

1247



1248

1249

Fig. 2. Variance reduction factor as a function of scale of fluctuation

1250

1251

1252

1253

1254

1255

1256

1257

1258

1259

1260

1261

1262

1263

1264

1265

1266

1267

1268

1269

1270

1271

1272

1273

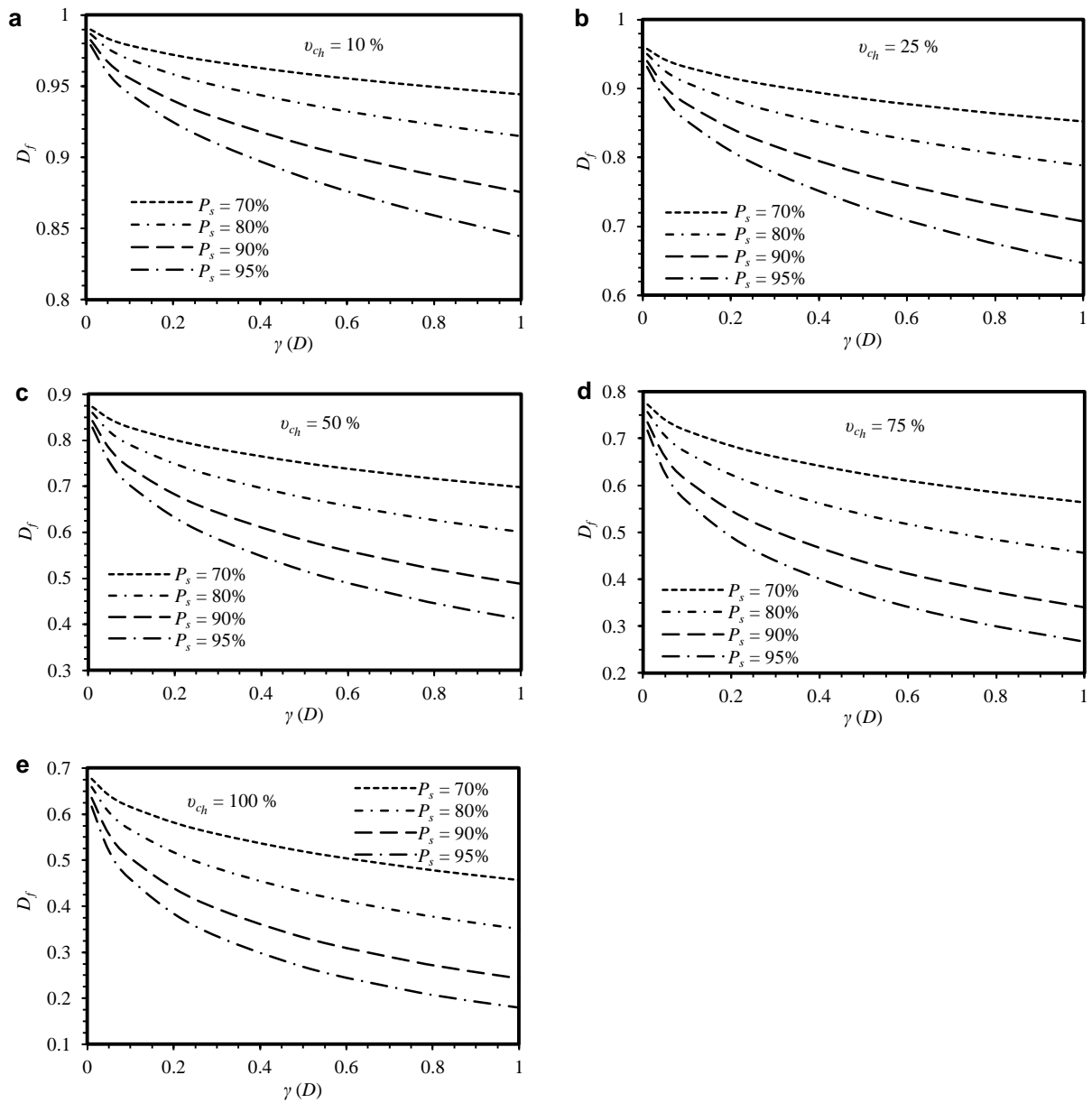
1274

1275

1276

1277

1278
1279
1280



1281
1282
1283
1284
1285
1286
1287
1288
1289
1290
1291

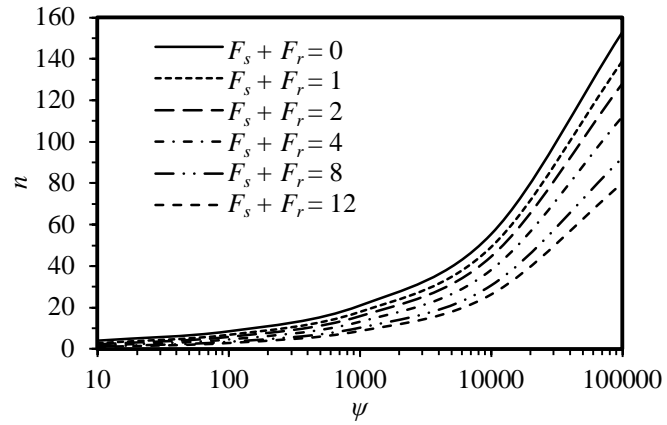
Fig. 3. Design factor D_f for (a) $\nu_{ch} = 10\%$; (b) $\nu_{ch} = 25\%$; (c) $\nu_{ch} = 50\%$; (d) $\nu_{ch} = 75\%$; (e) $\nu_{ch} = 100\%$

1292

1293

1294

1295



1296

1297

Fig. 4. Design graph for drain spacing [adapted from Zhou et al. (1999)]

1298

1299

1300

1301

1302

1303

1304

1305

1306

1307

1308

1309

1310

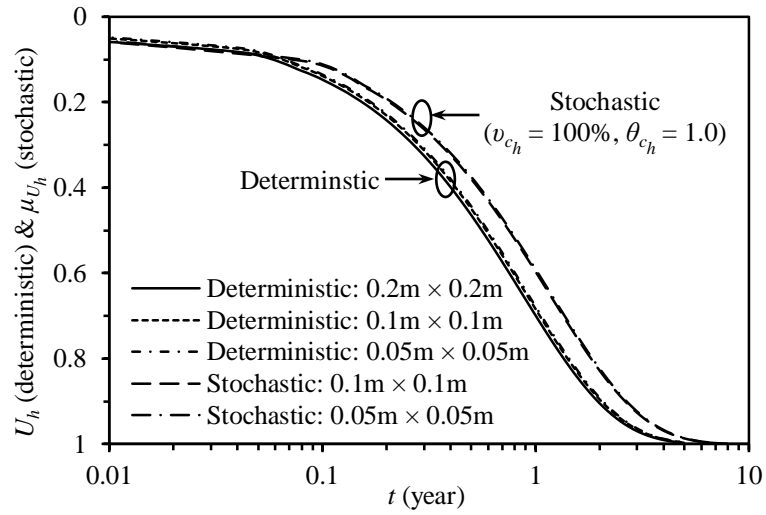
1311

1312

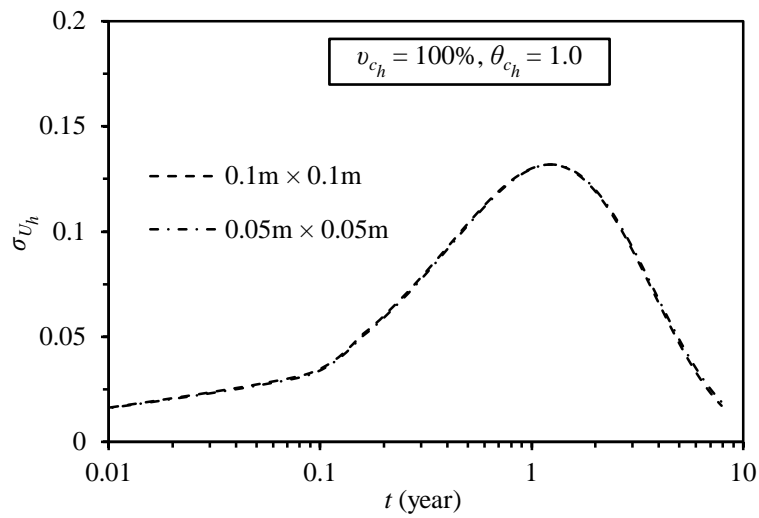
1313

1314

1315



(a)



(b)

1316

1317 **Fig. 5.** Influence of mesh density on: (a) U_h (deterministic) & μ_{U_h} (stochastic); (b) σ_{U_h}

1318

1319

1320

1321

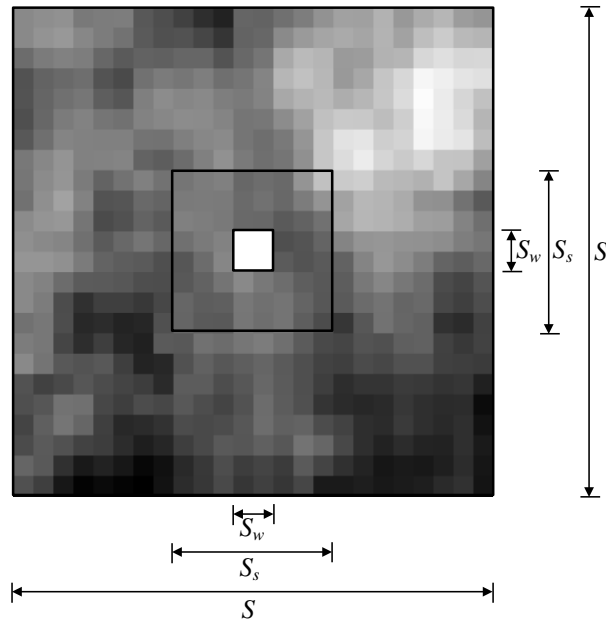
1322

1323

1324

1325

1326



1327

1328

1329

Fig. 6. Typical realization of the random field c_h with discretized finite element mesh

1331

1332

1333

1334

1335

1336

1337

1338

1339

1340

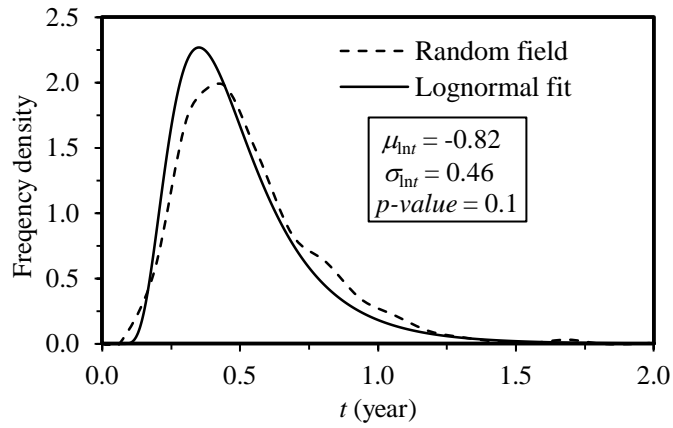
1341

1342

1343

1344

1345
1346
1347
1348
1349
1350



1351
1352

Fig. 7. Frequency density histogram and fitted distribution of t at $U_h = 88.1\%$ for $\nu_{c_h} =$

1353

$$100\%, \theta_{c_h} = 1.0$$

1354

1355

1356

1357

1358

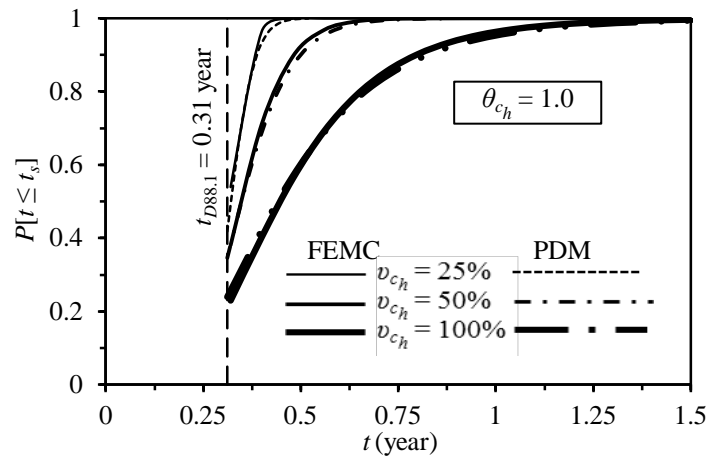
1359

1360

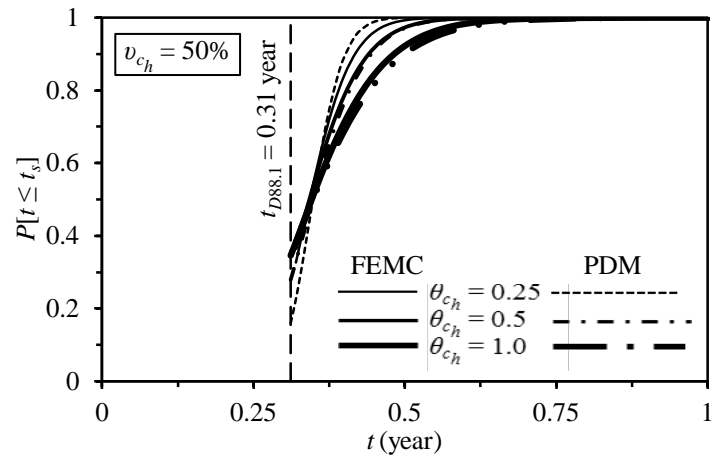
1361

1362

1363



(a)



(b)

1364

1365

Fig. 8. Comparison between FEMC and PDM for the effect of: (a) v_{c_h} on $P[t \leq t_s]$ for

1366

$\theta_{c_h} = 1.0$ and (b) θ_{c_h} on $P[t \leq t_s]$ for $v_{c_h} = 50\%$; at $U_h = 88.1\%$

1367

1368

1369

1370

1371

1372

1373